Local chemical order suppresses grain boundary migration under irradiation in CrCoNi

Ian Geiger [1], Penghui Cao [2,3], Timothy J. Rupert [1,2,4,5,*]

[1] Materials and Manufacturing Technology, University of California, Irvine, CA 92697, USA

[2] Department of Materials Science and Engineering, University of California, Irvine, CA 92697, USA

[3] Department of Mechanical and Aerospace Engineering, University of California, Irvine, CA 92697, USA

[4] Hopkins Extreme Materials Institute, Johns Hopkins University, Baltimore, MD 21218, USA

[5] Department of Materials Science and Engineering, Johns Hopkins University, Baltimore, MD 21218, USA

* Corresponding author: tim.rupert@jhu.edu

Supplementary Material

Supplementary Note 1

Given the elevated simulation temperature (1100 K), a natural question is whether the the grain boundary migration observed in Disordered boundaries arises solely from thermal annealing. To test this, three additional Disordered bicrystals (six grain boundaries total) were annealed for an extended period without displacement cascades. Fig. S1 compares Disordered boundaries under cascades (Fig. S1(a), reproduced from the main text) with those subjected only to annealing (Fig. S1(b)). Each cascade relaxation lasted ~36 ps (with minor variation from the adaptive timestep), providing a direct temporal comparison to the annealed samples. The annealed boundaries show only slight movement from their initial position over the long simulation, whereas irradiated boundaries fluctuate substantially. This demonstrates that the migration

observe under irradiation is not purely a thermal effect, though the high temperature likely enhances defect mobility within thermal spikes. Consequently, such boundary migration may not occur at lower temperatures, even under similar PKA bombardment.

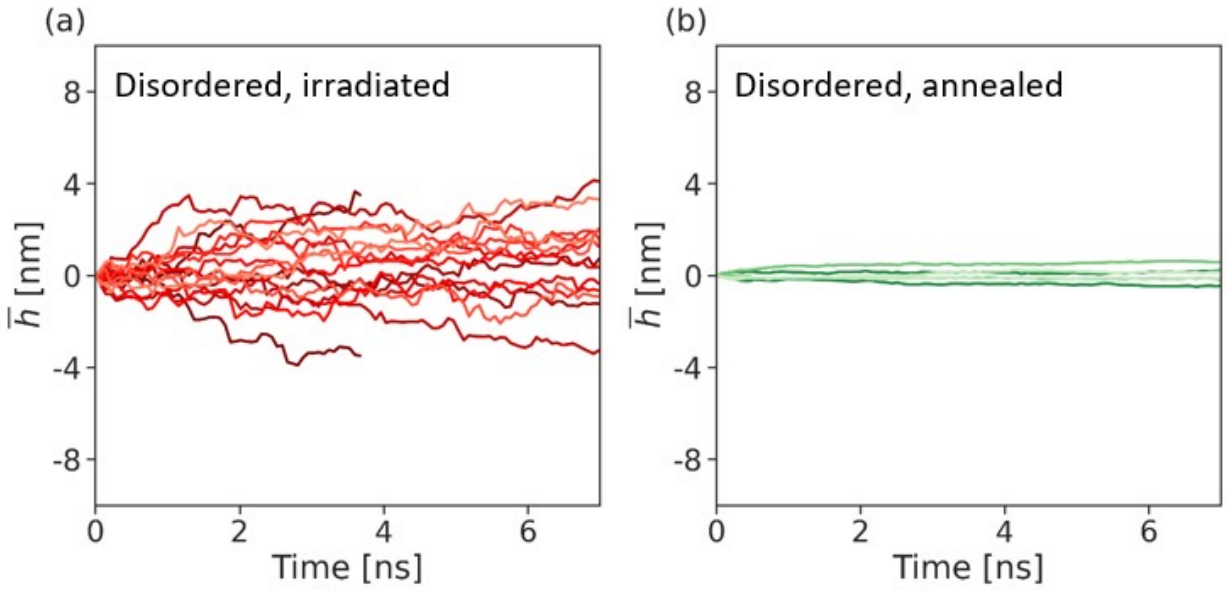

FIG S1. Average grain boundary displacement, $\bar{h}$, for each unique simulation in Disordered (a) irradiated and (b) annealed boundary sets. Line color denotes the specific grain boundary in each bicrystal.

Supplementary Note 2

Additional single-PKA simulations were performed to confirm the generality of the main text results. For each boundary, a randomly selected PKA was placed 5 Å from the interface and initiated with 5 keV of energy, directed normal to the boundary. As shown in Fig. S2, a large displacement cascade develops below each boundary within 2 ps, with distinct cascade morphologies stemming from the random nature of sub-cascade formation. By 20 ps, the defect region remains extensive, containing numerous vacancies and interstitials that produce pronounced waviness in the boundary by 30 ps. This behavior arises from atomic redistribution

near the interface, as many interstitials migrate to the boundary while vacancies accumulate into a cavity. In contrast, cascades in Segregated boundaries (Fig. S3) are, on average, smaller than in Disordered samples, as reflected by the mean boundary displacement, $\Delta\bar{h}$, and the standard deviation of atomic positions, σ. Snapshots at 20 ps and 30 ps show that the cascade region in Segregated samples rapidly contracts, leaving fewer point defects and producing only a minor disruption of the interface structure.

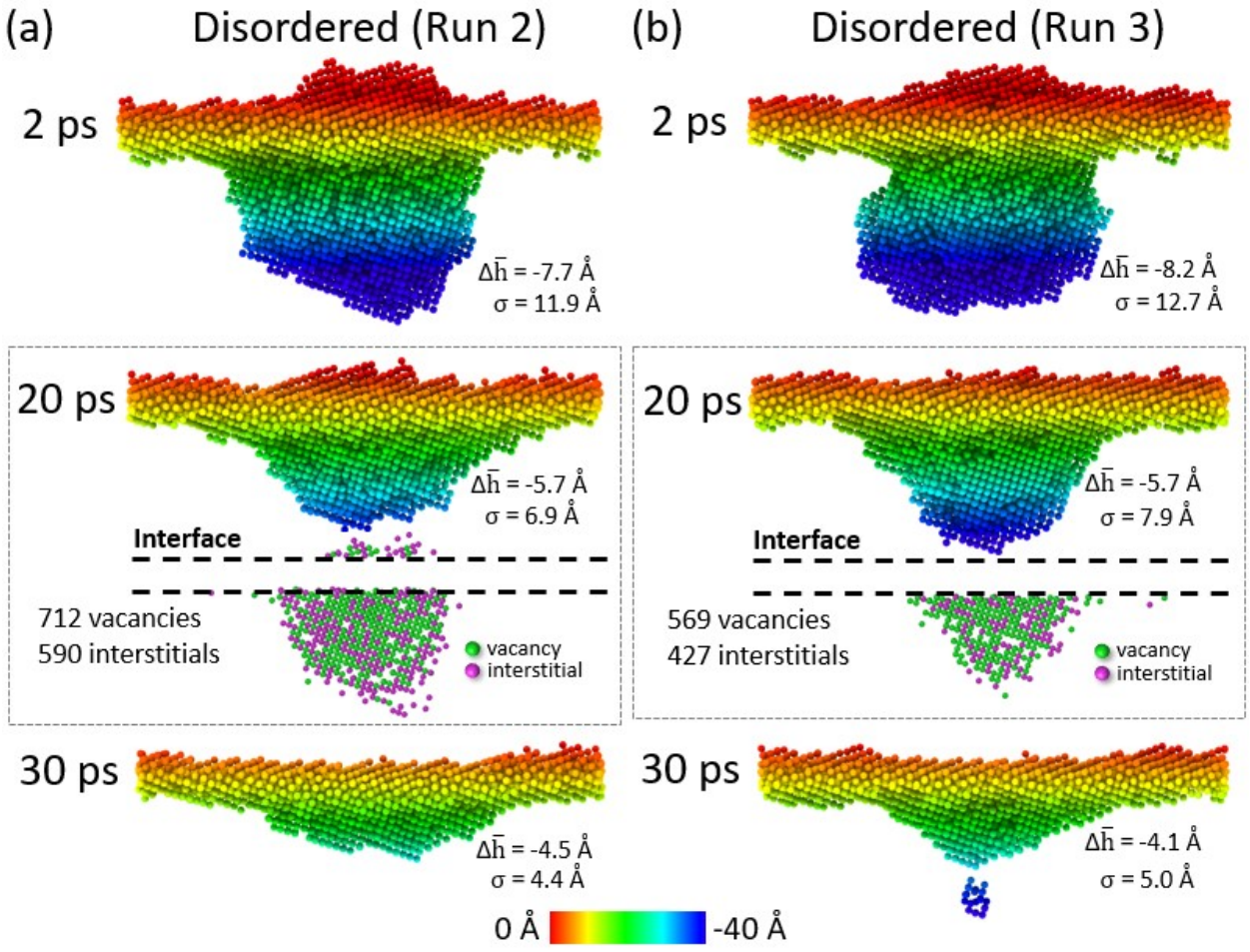

FIG S2. Evolution of single-PKA collision cascades during the thermal spike phase for two additional Disordered boundaries. Non-FCC atoms are shown and colored by depth after 2 ps, 20 ps, and 30 ps. At 20 ps, Wigner-Seitz cell analysis highlights point defect distributions and vacancy gradients. The mean boundary

displacement from the initial position, $\Delta\bar{h}$, and interfacial fluctuations, σ, are reported at each timestep to quantify migration and fluctuation behavior.

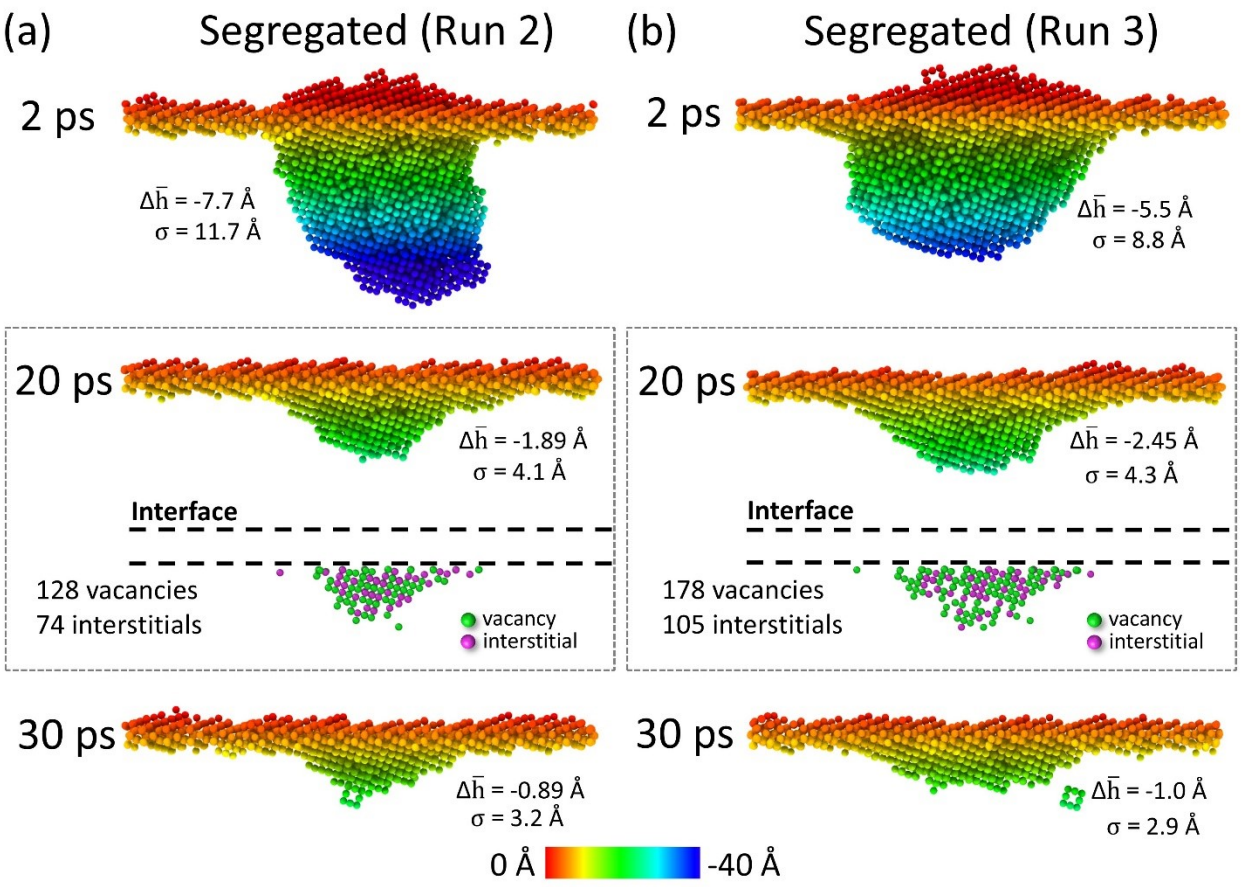

FIG S3. Evolution of single-PKA collision cascades during the thermal spike phase for two additional Segregated boundaries.